Atmospheric pressure dual RF–LF frequency discharge: transition from α to $\alpha - \gamma$ -mode

Romain Magnan, Gerjan Hagelaar, Mohamed Chaker, Françoise Massines

Atmospheric pressure dual RF-LF frequency discharge: transition from α to α-γ-mode

Romain MAGNAN[1,2], Gerjan HAGELAAR[3], Mohamed CHAKER[2] and Françoise MASSINES[1]*

[1]Laboratoire Procédés Matériaux et Energie Solaire, PROMES CNRS, UPR 8521, Rambla de la thermodynamique, 66100 Perpignan, France
[2] Institut National de la Recherche Scientifique, 1650 boulevard Lionel Boulet J3X1S2 Varennes, Canada
[3] Laboratoire plasma et conversion d'énergie, UMR5213, 118 Route de Narbonne, 31077 Toulouse, France
* Corresponding author, françoise.massines@promes.cnrs.fr

Abstract

This paper investigates the transition from α to α-γ-mode of a dual frequency (5 MHz/50 kHz) Dielectric Barrier Discharge (DBD) at atmospheric pressure. The study is based on both experiments and modelling of a plane/plane DBD in a Penning mixture (Ar-NH_3). The discharge is in the α-RF mode with three different voltage amplitudes (250, 300 and 350 V) and biased by a low-frequency (LF) voltage with an amplitude varying from 0 to 1300 V. At a given threshold of LF voltage amplitude (of about 400 V for a 2 mm gap and 133 ppm of NH_3), a transition from α to α-γ-mode occurs. It is characterized by a drastic increase of both the argon and NH emissions. Increasing the NH_3 concentration leads to a decrease of the LF voltage amplitude required to reach the α-γ-mode (experiment). The transition from α to α-γ-mode is initiated when the ionization in the sheath increases and the α-γ-mode is established when this ionization becomes higher than the self-sustainment criterion (1/ γ). The transition from α to α-γ-mode results in an increase of the particle densities and a stabilization of the gas voltage independently of the LF voltage amplitude. Without secondary electron emission there is no transition. In the model, increasing the secondary emission coefficient from 0.05 to 0.15 leads to a decrease of the LF voltage amplitude required to switch from α to α-γ-mode from 700 to 550 V.

Keywords: Dielectric barrier discharge (DBD), atmospheric pressure plasma, dual frequency

Introduction

Low Frequency (LF) Dielectric Barrier Discharges (DBDs) have many applications including ozone generation [1], polymer treatment [2], plasma medicine [3], air flow control [4], etc. Thin films of high quality are synthesized using diffuse, streamer-free, linear DBDs. Examples are water barrier [5]–[9] or passivating and antireflective layer for silicon photovoltaic cells [10]–[13] . The main advantage is an easy upscaling for large surface in-line coating. The DBD frequency was increased from kilohertz to megahertz to increase the power and thus the thin film growth rate [13], [14]. At radiofrequency (RF) α-RF mode, the discharge is sustained by the electrons generated in the gas bulk and the dielectric is not necessary to ensure discharge stability. However, highest power values are obtained in the γ-mode. In the γ-mode, the atmospheric pressure discharge tends to localize and a DBD configuration is helpful to achieve a diffuse discharge [15], [16]. At atmospheric pressure, the transition from α-mode to γ-mode is observed in RF discharges [17]–[19] as well as in dual RF-LF discharges [20]. According to the literature, there are two distinct ways to reach the transition: either increase the electric field into the sheath by increasing the voltage amplitude [17] or increase the secondary electron emission by applying a low frequency voltage able to transport the ions to the cathode [20]. Bischoff *et al* [18] studied the modification of the electron power absorption dynamics induced by changing the driving voltage amplitude and the N_2 concentration in atmospheric pressure plasma jets operated at 13.56 MHz in He/N_2 Penning mixture. Their experiments are based on phase resolved optical emission spectroscopy and their simulations are performed with a Particle In Cell (PIC) code including Monte Carlo treatment of collision processes (PIC MCC). Their plasma jets can operate in two different modes: the Ω- and the Penning-mode. In the Ω-mode, ionization occurs in the plasma bulk and reaches its maximum together with the current. Ionization results from the high electric field in the bulk. In the Penning-mode, the ionization maximum takes place at the sheath edge. Penning ionization occurs in the sheath. The electrons are accelerated by the sheath electric field and multiplied by collisions. The drift of the positive ions toward the cathode induces the emission of secondary electrons which are accelerated and multiplied collisionally in the sheath. Increasing the driving voltage leads to a transition from Ω- to Penning mode, the electrons generated in the sheath being accelerated and multiplied toward the bulk. Increasing the N_2 concentration by increasing the reactive gas flow induces a transition from Penning- to Ω-mode. This transition is attributed to an increase of the total pressure in the jet, which enhances the number of collisions.

In an atmospheric pressure dual frequency (DF) plasma (14 MHz– 2 MHz), increasing the voltage amplitude of the lower frequency component induces the increase of the electric field into the sheath. Ionization then takes place within the sheath and the transition from the α-mode to the γ-mode occurs [19]. The ionization mechanism shifts from wave riding to cathode secondary emission and the electron temperature increases.

Another way to induce the transition is by adding a low frequency (LF) voltage to a RF-DBD. In this case, the γ-mode is only reached for some microseconds when the LF voltage is maximum. The efficient transport of the ions towards the cathode induces a high secondary electron emission increasing the metastable production and the ionization in the sheath. This was for example observed by applying a 50 kHz voltage to a 5 MHz DBD in Ar/NH_3 mixture [20] or 200 kHz on 13.56 MHz [17]. In [20], for an LF voltage amplitude lower than some threshold, the increased ion loss to the cathode is not compensated by increased ionization and the plasma density thus decreases. For an LF voltage amplitude above the threshold, when the LF and RF cathode are the same electrode, the ionization in the sheath due to the multiplication of secondary electrons is high enough to counterbalance the ion loss and the discharge is γ-RF during 1/5 of the LF cycle. In this mode, the gas voltage is controlled by the charge of the dielectric like in a low frequency DBD. Around the gas voltage maximum, for each RF cycle, the discharge alternates between α-RF and γ-RF discharge. In this study, whatever the discharge mode, the mechanism governing ionization is Penning ionization.

To avoid confusion, given that the γ-mode occurs only during 1/5 of the LF cycle and that the discharge is in α-mode during the remaining time, we will denominate this regime as α-γ-mode in the following.

In this work, we use the same system/tools/model as before [20] to investigate the mechanisms involved in the transition between α-mode and α-γ-mode. For that purpose, the effect of the parameters that strongly influence the ionization rate are studied in the case of a RF-LF dual frequency DBDs in $Ar\text{-}NH_3$. These parameters are the amplitude of the RF and LF voltages and the NH_3 concentration in argon. As NH_3 is ionized by collisions with Ar metastable atoms, its concentration changes the ratio of direct ionization as compared to Penning ionization and the effective ionization level as well. Emission spectroscopy and fluid model results are presented and discussed in view to explain the reasons of the transition from α-RF to α-γ-RF. The model also allows studying the effect of the gamma coefficient.

Experimental set-up

The discharge cell and its power supply are schematically shown in **Figure 1**.

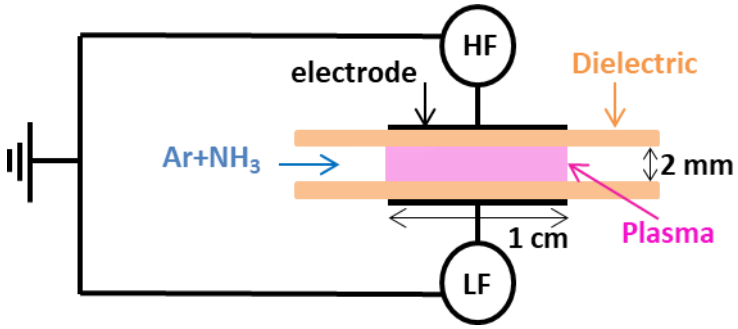

Figure 1. Schematic drawing of the discharge cell

As described in more details in a previous article [20], the DBD is a usual plane-to-plane DBD with each electrode powered by two different power supplies, one RF and one LF. These power supplies are synchronized. The frequencies of the two voltages are constant: 5 MHz and 50 kHz. Their amplitudes are independently adjusted. Three values (250, 300 and 350 V) are considered for the 5 MHz voltage (V_{RF}) while the 50 kHz voltage amplitude (V_{LF}) is varied from 0 to 1300 V.

The plasma is characterized by current and voltage measurements and by emission spectroscopy as described in [20]. The fluid model is also described in [20]. It solves the continuity and momentum transfert equations coupled to Poisson's equation for each species and the energy equation for electrons. Five species (Ar, electron, Ar^+, Ar_2^+, Ar*) and a simplified set of 10 equations are considered. The model was validated by the comparison with experimental power and Ar metastable densities measurements.

Results and discussion

The aim of this section is to understand the transition from α to α-γ-mode using the experimental and modelling results. The experimental results are focused on optical spectroscopy. The evolution of specific plasma emission lines as a function of the LF voltage for the three RF voltage values are discussed. Subsequently, the effect of the NH_3 concentration on the voltage values at the transition from α to α-γ-mode are presented. Then, the modelling results for similar voltage values are discussed to explain the transition. These results include the ionization into the sheath, the mean particle densities, the gas voltage, the power absorbed per electron and the consequence of the secondary electron emission coefficient.

1. Experimental results

Our previous study [20] showed that in the experimental conditions used in the present work, the DF-DBD is in the α-mode when RF is 5 MHz-350 V and LF is 50 kHz-400 V. It is in the α-γ-mode for RF at 5 MHz-350 V and LF at 50 kHz-1000 V. Emission spectra observed in these two conditions are shown in **Figure 2.** This figure illustrates the main similarities and differences between the emission spectra of α and α-γ-DF-DBD modes.

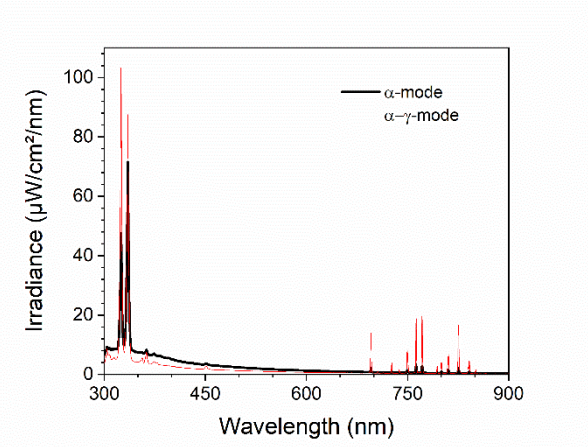

Figure 2. DF-DBD plasma irradiance for RF at 5 MHz-350 V and for a) LF at 50 kHz-400 V (α-mode) and b) LF at 50 kHz-1000 V (α-γ-mode)

The emission lines and bands present in the spectra are the same whatever the discharge mode. In both modes, the emission band of NH at 324 and 336 nm and the argon emission occurring between 696 nm and 900 nm are found. The continuum emission characteristic of an RF discharge at atmospheric pressure is also always observed. The amplitudes of these different emissions only depend on the discharge mode.

When switching from α-mode to α-γ-mode, the two NH emissions increase and their ratio changes in such a way that the 324 nm becomes dominant. The argon emissions sharply increase. The continuum intensity principally attributed to Bremsstrahlung decreases while its shape does not change. These changes can be related to an increase of the electron energy; indeed, the excitation energy threshold for the upper level of the NH 324 nm transition (5.42 eV) is higher than that of the NH 336 nm transition (3.69 eV). Moreover, high electron energy (13 eV) is needed to excite argon energy levels from the ground level. The transition from DF-DBD α-mode to DF-DBD α-γ-mode results in an increase of all the emission lines or bands requiring highly energetic electrons. This is in agreement with the results of numerical modelling presented in [20] showing that the transition from α to α-γ-mode induces an increase by a factor 3 of the mean argon metastable density which is the average on time and space. The Penning reaction is responsible for 95 % of the ionization in the α-mode and to 80 % in the α-γ-mode, while direct ionization increases from 0 to 15 %. In view these different emission spectra for the α and α-γ-modes, the amplitude of the Ar lines at 750 nm and at 811 nm and of the NH band at 324 nm can be used to understand the effect of both RF and LF voltage amplitudes and NH_3 concentration on the discharge mode transition. The argon lines at 750 nm and 811 nm are due to the transitions $2p_1 \rightarrow 1s_2$ and $2p_9 \rightarrow 1s_5$, respectively. The $2p_1$ level is mainly populated by electron excitation from the $^1S_0$ ground state (0 eV) of argon and the $2p_9$ level (13.08 eV) from the $1s^5$ metastable level (11.55 eV) [21], [22]. The argon line at 750 nm therefore provides information on the density of high-energy electrons (>11.55 eV) whereas the 811 nm mainly depends on the densities of argon metastable atoms and lower-energy electrons. The NH band at 324 nm is related to the lower-energy electrons. Previous studies [14] have shown that in RF-DBD the Ar emission is more localized close to the cathode sheath. **Figure 3** presents the evolution of the argon line intensity at 750 nm and 811 nm and of the NH band at 324 nm as a function of the V_{LF} for three V_{RF}, namely 250, 300 and 350 V. The discharge is initiated with 133 ppm of NH_3. There is a sharp increase of all emissions for V_{LF} above 400 V. This is in agreement with the variation with V_{LF} of the average and maximum light intensity measured from 450 to 800 nm with a photomultiplier and of the current measurement presented in [20]. These measurements were related to the variation of the average electron and ion densities calculated by the model and attributed to the transition from α-RF mode to α-γ-RF mode. **Figure 3** shows that whatever the V_{RF}, this transition occurs for the same value of V_{LF}. In other words, V_{RF} does not influence the transition from α-mode to α-γ-mode.

a) b)

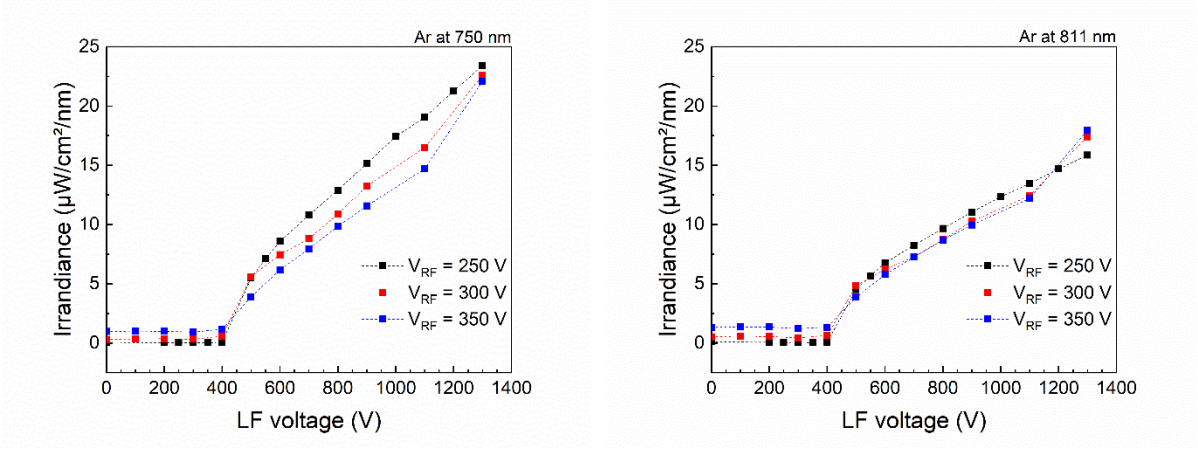

c)

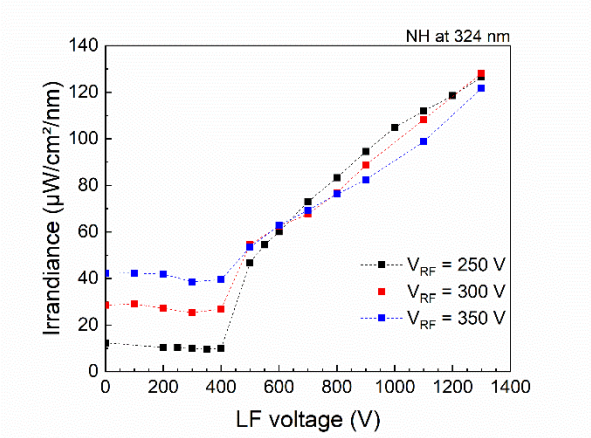

Figure 3. Variation of the emission intensity as a function of the LF voltage amplitude for V_{RF} = 250, 300 and 350 V of a) Ar line intensity at 750 nm, b) Ar line intensity at 811 nm, c) NH band intensity at 324 nm

Up to V_{LF} = 400 V, i.e. in the α-mode the NH band intensity significantly increases with V_{RF}, while the Ar lines are weakly influenced. This could be explained by the increase of bulk plasma density in the α-mode. Furthermore, increasing V_{LF} leads to a slight decrease of the three lines until the 400 V threshold value. Beyond, all sharply increase with V_{LF}. After the intensity jump, the NH emission remains about the same at any V_{RF} which implies that the jump is higher at low V_{RF} values. Another aspect is that the emission intensity of the Ar line at 750 nm, which largely depends on high energy electrons, is lower for higher V_{RF} in the α-γ-mode.

According to these emission spectroscopy results, the V_{RF} voltage does not influence the transition from α to α-γ-mode, even if the voltage applied to the electrodes is the sum of V_{RF} and V_{LF}. To understand why the effect of the V_{RF} amplitude is so negligible on the V_{LF} transition threshold between α and α-γ-modes, the concentration of NH_3 was varied. It could indeed be a

key factor influencing the effective ionization frequency of the gas. In RF-DBD, Penning ionization ($Ar^* + NH_3 \rightarrow Ar + NH_3^+ + e^-$) plays a significant role. According to our previous results [20], its contribution to ionization is 95% in the α-mode and 80% in the α-γ-mode. A well mastered solution to increase the ionization is to increase the NH_3 concentration.

Figure 4 presents the dependence on the NH_3 concentration of the LF voltage threshold leading to the transition from α-mode to α-γ mode (Fig. 4a) and of the RF-DBD voltage breakdown (Fig. 4b). The V_{LF} threshold values reported in **Figure 4a** correspond to the jump location for the NH and Ar emissions, which is the signature of the transition from α to α-γ-mode. V_{RF} was kept at 300 V for these measurements as this value ensures to always ignite the discharge provided the NH_3 concentration is higher than 10 ppm. Otherwise, this voltage is too low to achieve a RF-DBD without NH_3.

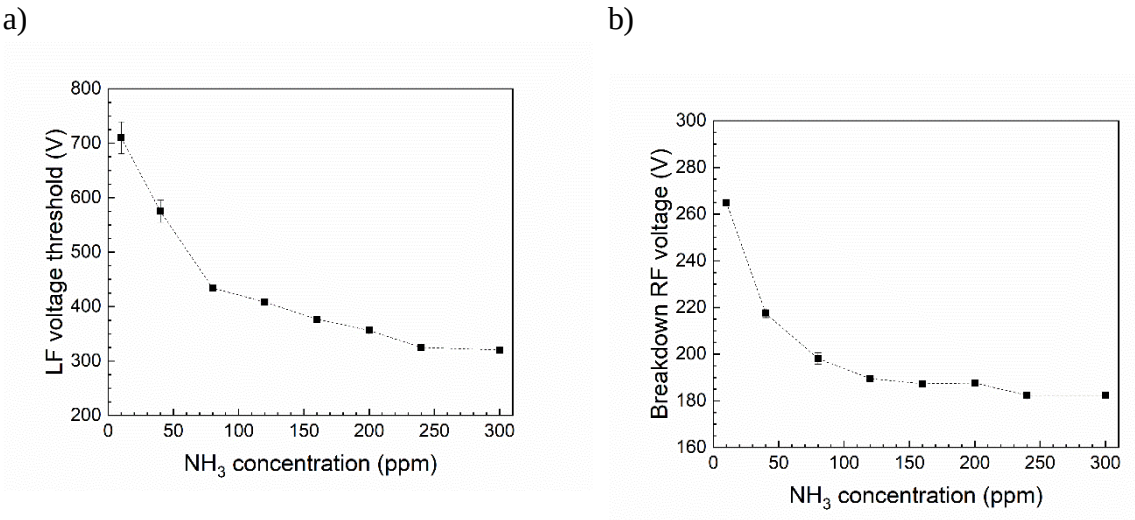

Figure 4. Effect of NH_3 concentration on a) the LF voltage value at the transition between α and α-γ-modes for V_{RF} = 300 V b) the breakdown voltage of the RF DBD (5 MHz)

As presented in **Figure 4b**, the breakdown voltage of the RF-DBD drastically decreases when the NH_3 concentration increases from 10 to 120 ppm. For higher concentrations, the breakdown voltage is almost constant showing that Penning ionization is more limited by the concentration of Ar metastables than the NH_3 concentration. The voltage threshold yielding the switch from α to α-γ-modes is presented in **Figure 4a** as a function of the NH_3 concentration. It clearly decreases with the NH_3 concentration, particularly for concentrations lower than 120 ppm suggesting that the larger multiplication of the electrons due to Penning ionization which decreases the breakdown voltage, also decreases the threshold between α and α-γ-modes.

In conclusion, according to these experimental results, the transition from α to α-γ-modes depends on both the V_{LF} amplitude and the NH_3 concentration but not on the V_{RF} amplitude. At

a first glance, we can consider that V_{LF} controls the secondary emission of electrons from the cathode and NH_3 the ionization. Thus, the transition depends on the flux of secondary electrons emitted from the cathode and especially their multiplication into the sheath. In the next section, the simulation results are presented to complete the experimental study and to shed light on the mechanisms governing the transition from α to α-γ-modes.

2. Modelling results

The modelling study was carried out for the conditions used in the experiment: V_{LF} varying from 0 to 1300 V, three V_{RF} values: namely 250, 300 and 350 V and a NH_3 concentration of 200 ppm. The secondary electron emission coefficient (γ) was varied from 0 to 0.15.

2.1 - Comparison of experimental and modeling results

The variation of the mean densities of electrons (n_e) and Ar* (n_{Ar^*}) and their ratio as a function of the LF voltage amplitude are presented in **Figure 5** for V_{RF} = 250, 300 and 350 V and γ = 0.10. These densities are the average over the gap distance and a LF cycle.

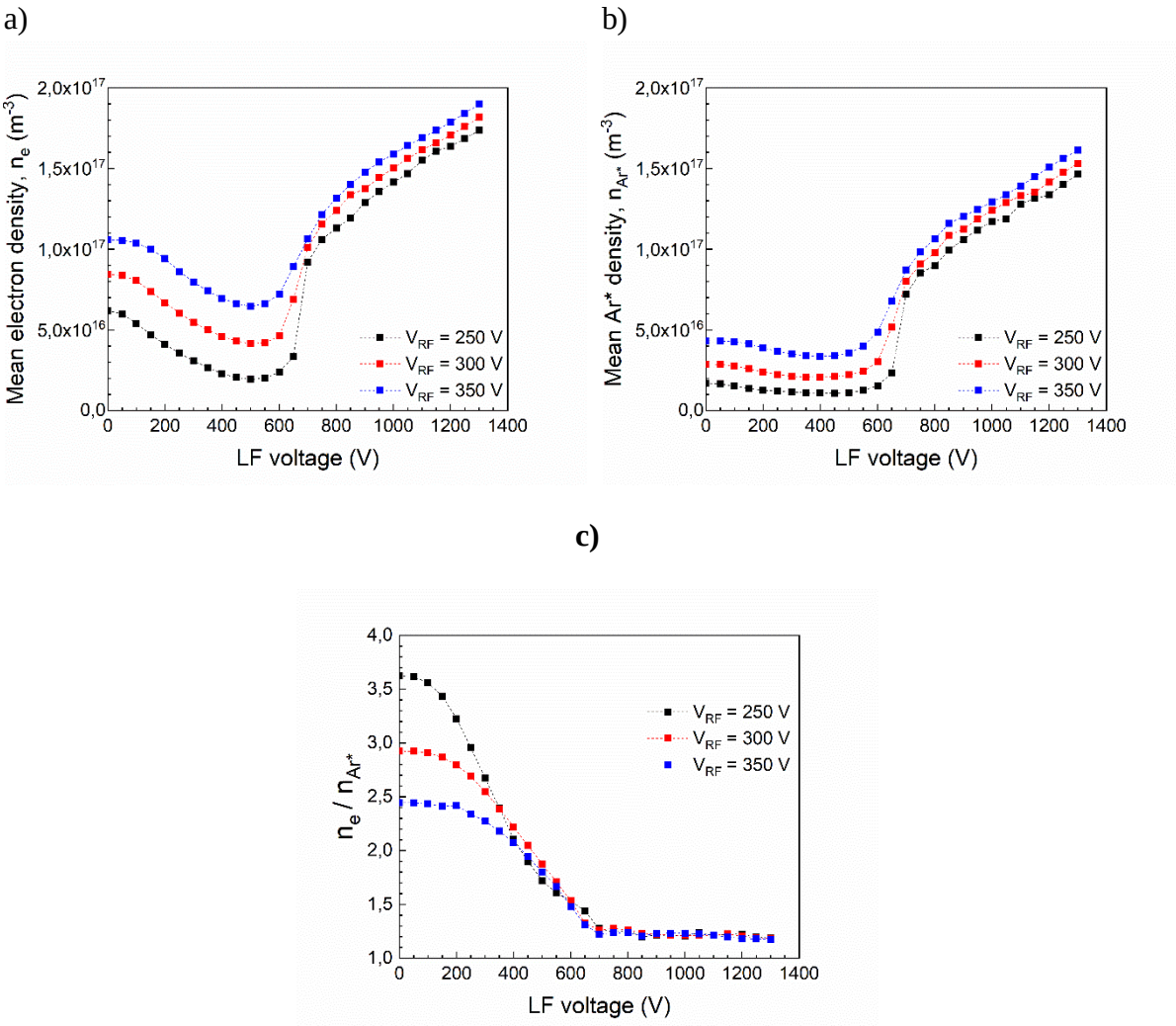

Figure 5. Variation as a function of the LF voltage amplitude for V_{RF} = 250, 300, 350 V and γ = 0.10 of a) the mean density of electron (n_e) b) the mean density of Ar metastable (n_{Ar^*}) and c) the ratio of the mean density electrons and the Ar metastable

Figure 5a-b shows that in the α-mode the densities increase with V_{RF}. The behavior of electron and metastable densities are similar, with a transition around V_{LF} = 500 V for the three V_{RF} values. Below 500 V, all the densities decrease with increasing the LF voltage due to the

uncompensated ion losses, large enough to reduce the RF power. Between 500 and 700 V both densities drastically increase. The electron density is enhanced by a factor of 2 to 5 and the Ar* density by a factor of 2 to 6, depending on V_{RF}, the increase being larger for the lower V_{RF}. Moreover, the influence of V_{RF} is larger below the transition. The drastic increase of the electron and metastable density above 500 V might be due to an additional γ-breakdown which induces the electron multiplication into the sheath, thus explaining the increase of the mean particle densities. Above 700 V the densities increase linearly with V_{LF}. The larger V_{RF}, the larger the densities are. However, this effect is significantly smaller for the α-γ-mode than for α-mode. These variations are similar to the variation of the measured intensity of the Ar and NH emissions presented in **Figure 3**. According to emission spectroscopy and modeling results (i) the V_{LF} value at the transition is independent of V_{RF}, (ii) during the α-mode, V_{RF} affects the discharge as clearly observed on NH emission and mean particle densities, and (iii) in the α-γ-mode, the emissions and the mean densities increase linearly with V_{LF}.

According to **Figure 5c**, the ratio of the electron to metastable densities also clearly illustrates the transition from α to α-γ-mode. The density of electrons is always larger than that of Ar metastables. The difference is smaller (ratio close to 1 in the α-γ-mode while it varies from 3.5 to 2.5) when V_{RF} decreases from 350 to 250 V. From about V_{LF} = 200 V, the difference decreases in the DF-DBD to reach a ratio independent of V_{RF} around V_{LF} =400 V. The ratio continues to decrease until the transition ends at about 700 V whatever V_{RF}. Then it stabilizes at 1.2 e/Ar* once the α-γ-mode is established.

One may wonder why the V_{LF} value at the transition from α to α-γ-modes does not depend on the V_{RF} amplitude in our case. The behavior of a DBD depends on the voltage applied to the gas (V_g) defined by the difference between the voltage applied to the electrodes ($V_a = V_{RF} + V_{LF}$) and that applied to the dielectrics (V_{ds}). **Figure 6a** presents the variations of V_a, V_g and V_{ds} over a LF cycle in the α-mode (RF at 5 MHz-350 V and LF at 50 kHz-400 V). In this case, the charge on dielectrics is low and V_a and V_g are thus similar. However, in the α-γ-mode (RF at 5 MHz-350 V and LF at 50 kHz-1000 V), according to **Figure 6b**, V_g drastically decreases once the γ-mode is reached because of the drastic increase of the discharge current. Thus, V_g rather than V_a should be considered to understand the discharge behavior.

a) b)

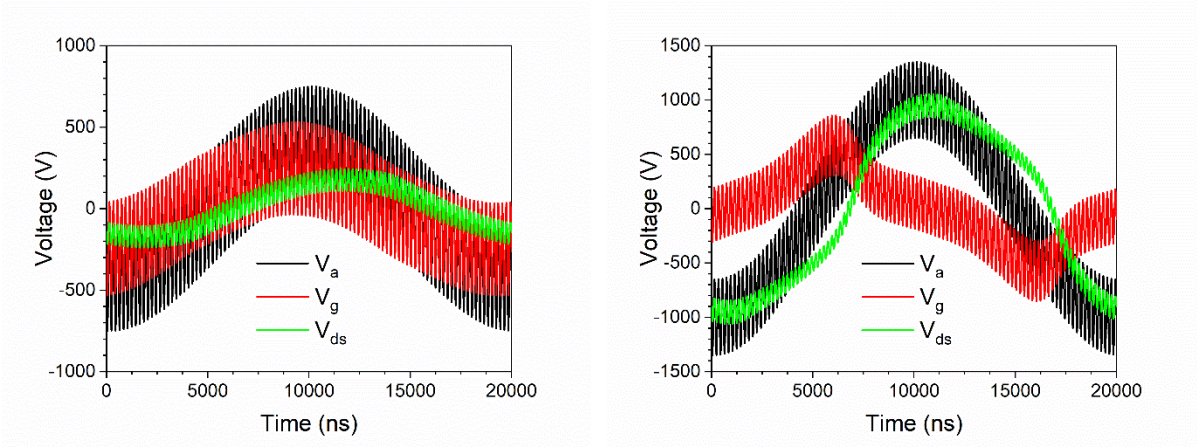

Figure 6. time-dependence of the voltage applied to the electrodes (V_a), on the voltage across the gas gap (V_g), and the voltage applied to the dielectrics (V_{ds}), over one LF cycle for discharge in a) α-mode (RF at 5 MHz-350 V and LF at 50 kHz-400 V) and b) α-γ-mode (RF at 5 MHz-350 V and LF at 50 kHz-1000 V)

Figure 7 shows the gas voltage (V_{gMax}) maximum as a function of V_{LF} for V_{RF} = 250, 300 and 350 V and γ = 0.10.

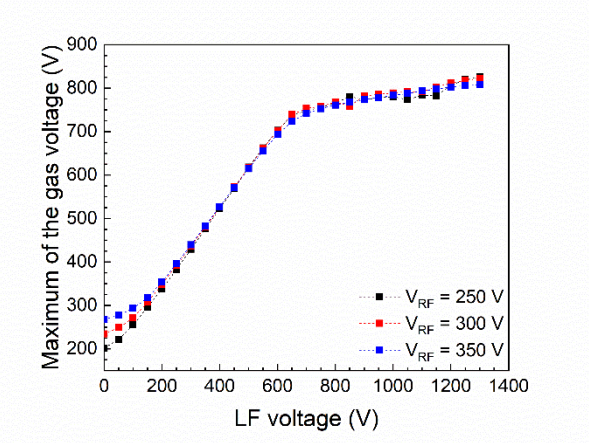

Figure 7. Variation of the maximum of the gas voltage for V_{RF} = 250, 300 and 350 V and γ = 0.10 as a function of the LF voltage amplitude

V_{RF} has only an influence from 0 to 200 V. From 200 V to 600 V, V_{gMax} is multiplied by a factor of 2. As the dielectrics used in our experiments have a dielectric permittivity ε = 9, the corresponding larger charge on the dielectrics induces a larger V_{ds} voltage explaining why V_{RF} does not modify V_{gMax}. For V_{LF} values above 600 V, V_{gMax} only slightly increases to reach about 800 V, showing that the γ-mode occurs for a constant V_{gMax} value which is independent of V_a. This behavior indicates that the discharge turns into γ-mode as soon as the gas voltage value allows the γ-breakdown. In this mode the current is large enough to rapidly increase V_{ds} and to decrease V_g. This behavior is the usual behavior of a low frequency DBD as shown in [20].

The influence of the γ secondary emission coefficient on the maximum of the gas voltage is illustrated in **Figure 8** for γ = 0, 0.05, 0.10 and 0.15 at the highest V_{RF} value considered in this work, namely 350 V, using γ = 0 as a reference.

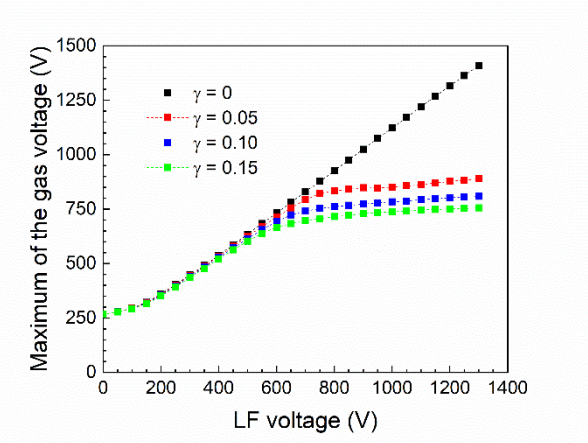

Figure 8. Variation of the maximum of the gas voltage for γ = 0, 0.05, 0.10, 0.15 and V_{RF} = 350 V as a function of the LF voltage amplitude

As expected, in the α-mode no effect of the γ coefficient on V_{gMax} occurs. In the α-γ-mode, V_{gMax} slightly decreases when the secondary electron emission coefficient increase. The transition also occurs for lower V_{LF} from700 V to 550 V for γ increase from 0.05 to 0.15. Without secondary electrons, no transition from α to α-γ-mode takes place.

2.2 - Contribution of the different ionization mechanisms

We consider that the ionization mechanisms comprise ionization in the plasma bulk, sustained by ohmic heating by the electron current in the bulk, and ionization in the sheath due to the multiplication of secondary electrons emitted from the wall. The sheath oscillates with the RF voltage and is modulated by the LF voltage and (in the α-γ regime) by the γ-breakdown. To separate the bulk from the sheath ionization at any time, we consider that the sheath region is characterized by $n_e/n_i \ll 1$ and the bulk region by $n_e/n_i \geq 1$. Hence we split the spatial profile of the electron source term $S(x)$ (number of ionizations per unit volume and per unit time, as a function of position x) into two contributions as follows:

$$S(x) = S_{sheath}(x) + S_{bulk}(x) \quad \textbf{(1)}$$

$$S_{sheath} = S \max\left(1 - \frac{n_e}{n_i}, 0\right) \quad \textbf{(2)}$$

$$S_{bulk} = S \min\left(\frac{n_e}{n_i}, 1\right) \quad \textbf{(3)}$$

In these equations, the source term is multiplied by space-dependent weight functions, equation (2) and (3), varying between 0 and 1 with a smooth transition around the sheath edge; the max and min limiters are included to prevent negative values of S_{sheath} in the plasma bulk (in case $n_e > n_i$). The total sheath ionization rate per wall surface area is:

$$\Gamma_{sheath} = \int_{x_{wall}}^{x_{max}} S_{sheath}(x)dx \quad \textbf{(4)}$$

The integration is from the wall to the position of the maximum electron density. Note that the upper integration limit is not very important, as long as it is located within the plasma bulk where the spatial profile of S_{sheath} has dropped to zero. In a similar way, the total bulk ionization rate per wall surface area Γ_{bulk} is obtained by integrating S_{bulk} between the walls. These integrated ionization rates can be compared directly with the flux of secondary electrons emitted from the wall surface, Γ_{wall}.

The total ionization rate in the sheath, as defined by the equations above, may not be caused completely by secondary electrons that cross the sheath but could also have a (small) contribution from the plasma bulk, especially near the sheath edge. In fact, the separation into sheath and bulk is not well defined. Therefore, the sheath ionization rate shown later should be regarded as an upper limit for the ionization of the secondary electron avalanche.

The time variation of the total electron production rate (integrated) in the bulk (Γ_{bulk}), in one of the sheaths (Γ_{sheath}) and at one of the walls (Γ_{wall}) over one LF cycle, for $\gamma = 0.10$ is presented

in **Figure 9a** for the α-mode (RF at 5 MHz-300 V and LF at 50 kHz-400 V) and in **Figure 9b** for the α-γ-mode (RF at 5 MHz-300 V and LF at 50 kHz-1000 V). The results in this figure have been averaged over the RF cycles.

a) b)

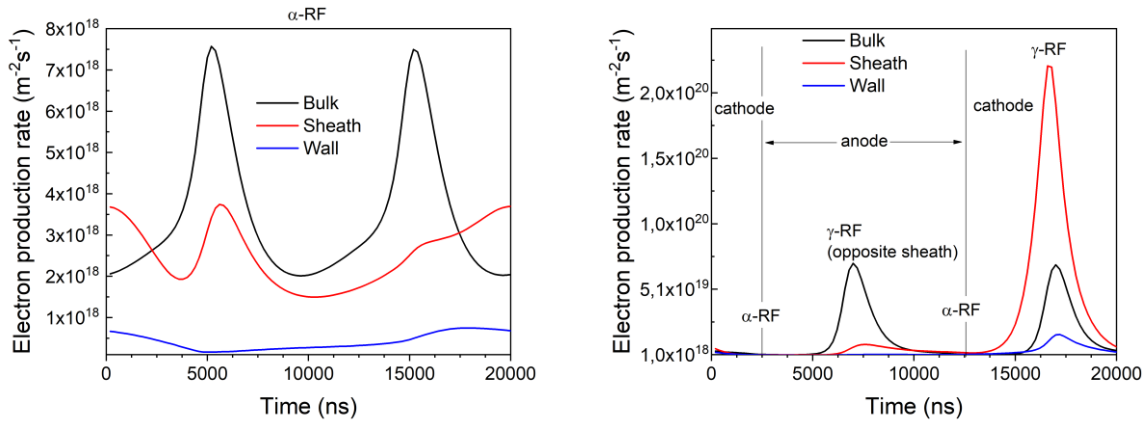

Figure 9. Electron production rate in the bulk, in one of the sheaths and at the corresponding wall over one LF cycle, averaged on a RF cycle with γ = 0.10 for a) α-mode (RF at 5 MHz-300 V and LF at 50 kHz-400 V) and b) α-γ-mode (RF at 5 MHz-300 V and LF at 50 kHz-1000 V). Anode and cathode indicate the wall polarity.

In the α-mode, the secondary emission is low compared to the ionization in the sheath and in the plasma bulk. In the αγ-mode, when the discharge is γ-RF, the ionization in the cathode sheath exceeds that in the bulk and the bulk ionization maximum is ten time larger than in the α-RF. At its maximum, the ionization occurs in the bulk for the α-mode, and in the sheath for the α-γ-mode.

It is well known in gas discharge physics [23] that the cathode sheath becomes self-sustained if each secondary electron produces enough ions in the sheath to cause the emission of one or more new secondary electrons. The criterion to determine if the ionization in the sheath is large enough to induce a self-sustained discharge is defined as:

$$\frac{\langle \Gamma_{sheath} \rangle_{RF}}{\langle \Gamma_{wall} \rangle_{RF}} > \frac{1}{\gamma} \quad \textbf{(5)}$$

with RF-averaged quantities defined as :

$$\langle X \rangle_{RF}(t) = \frac{\omega_{RF}}{2\pi} \int_{-\pi/\omega_{RF}}^{\pi/\omega_{RF}} X(t+t')dt' \quad \textbf{(6)}$$

where ω_{RF} is the angular RF frequency. The criterion is defined with values averaged over one RF cycle because the self-sustainment mechanism involving ion transport back to the wall is too slow to react to the RF fluctuations of the electric field in the sheath.

The left hand side of the criterion (5) can be understood as the average number of ionizations in the sheath per secondary electron emitted. **Figure 10** shows the maximum of this parameter, defined as the ratio of the maximum value of the sheath ionization rate $\langle \Gamma_{sheath} \rangle_{RF}$ that occurs during the LF cycle, to the maximum secondary electron flux $\langle \Gamma_{wall} \rangle_{RF}$ emitted from the wall during the cycle. This ratio is shown as a function of the LF voltage and compared with 1/γ for different γ (0.05, 0.1 and 0.15) and V_{RF} (250, 300 and 350 V) values. The threshold for self-sustained sheath is indicated by a horizontal line in each figure, labeled 1/γ. In the α-γ mode, the ionization per secondary electron is significantly higher than 1/γ (expected for a self-sustained sheath in equilibrium) which is certainly related to the uncertainty on the sheath width.

a)

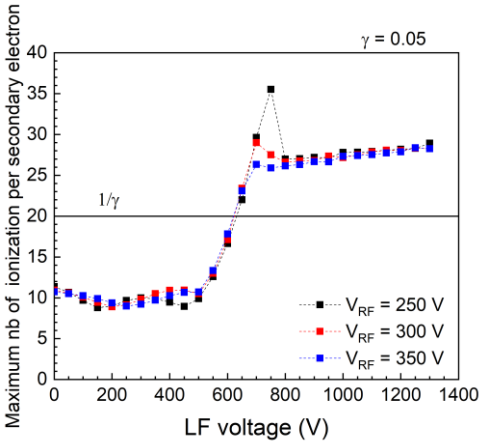

b)

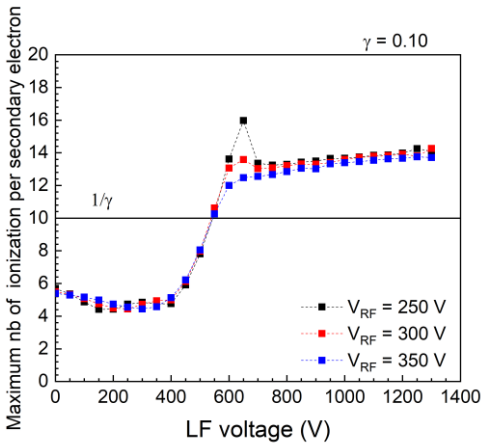

c)

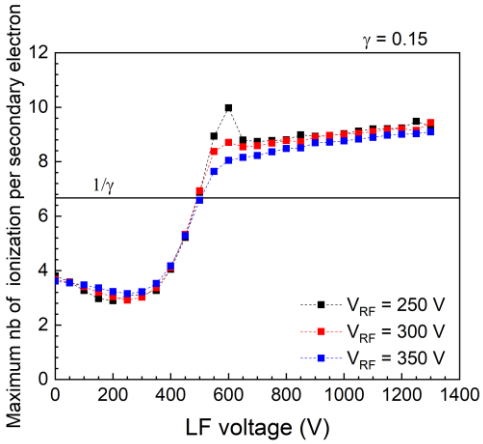

Figure 10. Maximum number of ionizations per secondary electron (ratio of maximum sheath creation to maximum wall creation) for V_{RF} = 250, 300 and 350 V as a function of the LF voltage amplitude for a) γ = 0.05 b) γ = 0.10 and c) γ = 0.15

Whatever the secondary electron emission coefficient, the maximum number of ionizations per secondary electron almost follows the same shape as a function of the LF voltage and is independent of the RF voltage. Three zones are observed that clearly correspond to the α-mode, to the transition and to the α-γ-mode.

In the α-mode at low V_{LF}, there is not enough ionization for a self-sustained sheath, but beyond some V_{LF} value, the ionization in the sheath rapidly increases until the self-sustainment criterion is met at least at some time during the LF cycle. This transition from a non-self-sustained to a self-sustained sheath explains the observed transition of the discharge from the α-mode to the α-γ-mode

For a given γ, the ionization curves in **Figure 10** are almost independent of the RF voltage amplitude as it was the case of the gas voltage maximum in **Figure 7**. This suggests that this maximum gas voltage controls the RF-averaged ionization rate in the sheath.

Table 1 summarizes the effect of the γ value on the V_{LF} value at the transitions: the maximum V_{LF} of α-mode, the threshold V_{LF} for achieving a self-sustained sheath and the minimum V_{LF} for α-γ-mode. This latter V_{LF} voltage has been obtained from **Figure 10** and it corresponds to the value after the overshoot. In the α–γ-mode, the maximum number of ionizations per secondary electron remains constant. These values are reported in the **Table 1**.

Table 1. Effect of the γ value on the VLF values at the transition

γ	V_{LF} max of α-mode (before the transition)	V_{LF} to reach the self-sustained criteria (1/γ)	V_{LF} min of α-γ-mode	(maximum number of ionizations per secondary electron for V_{LF} min of α-γ-mode mode) x (γ)
0.05	500 V	~ 625 V	800 V	27x0.05 = 1.35
0.1	400 V	550 V	700 V	13.5x0.1 =1.35
0.15	300 V	500 V	650 V	9x0.15 = 1.35

Whatever the γ value, increasing the LF voltage amplitude leads to a drastic increase of the maximum number of sheath ionizations per secondary electron in the sheath, until it is higher than the self-sustained criteria (1/γ). Thus, in a α-γDBD, the sheath is self-sustained. The

transition from α to α-γ-mode is related to the ionization level in the sheath. This is in agreement with experimental results showing that the LF voltage transition decrease with the increase of the NH_3 concentration. Penning ionization is the dominant ionization mechanism and it increases with NH_3 concentration.

Figure 11 illustrates the consequences of sheath self-sustainability on the different average plasma particle densities. The consequence of varying the secondary electron emission coefficient on the mean value of electron, ion and Ar metastable densities is presented in **Figure** 11 for V_{RF} = 350 V.

a) b)

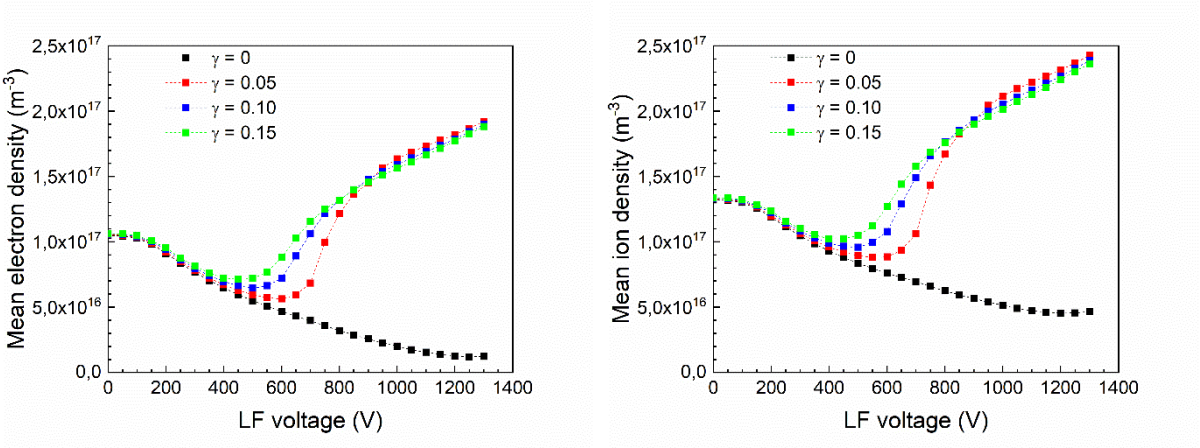

c)

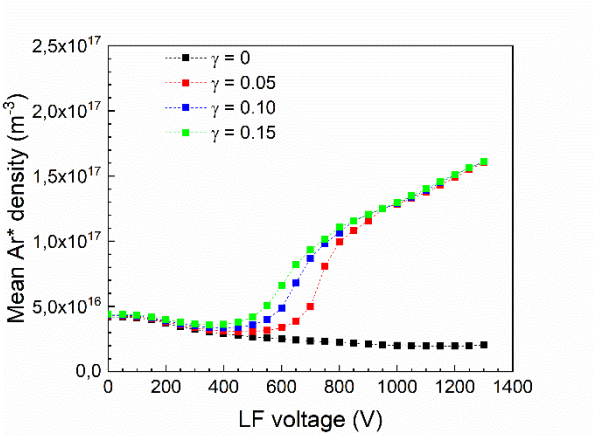

Figure 11. Variation as a function of LF voltage for γ = 0, 0.05, 0.10 and 0.15 and V_{RF} = 350 V of the mean densities of a) electron b) ion and c) Ar*

In the α-mode, the γ coefficient has no influence on any of the densities, as it was the case for the gas voltage maximum. However, at the transition from α to α-γ-mode, between 400 and 800 V, all the densities are significantly dependent on the secondary electron emission coefficient.

Without secondary electron emission, the mean average densities monotonously decrease until the discharge turns off for V_{LF} higher than 550 and 900 V when V_{RF} = 250 and 300 V, respectively.

The contribution of the secondary electron emission induces an increase of the densities which, for V_{LF} = 1300 V, reaches a factor of 15 for the electrons, of 5 for the ions and of 8 for the Ar metastable. Although for the same ion flux, the variation of the γ coefficient from 0.05 to 0.15 increases the electron flux from the cathode by a factor of 3, it only slightly increases the mean average electron and ion density and has no influence on the metastable atom density. This is explained by the decrease of V_{gMax} during the γ-mode which decreases the creation of metastable atoms and the gas ionization. An additional explanation is that the γ-mode occurs only during 1/5 of the LF cycle.

2.3 - RF versus LF power

The variation of the power absorbed per electron is also a typical parameter witch informs on the modification of the discharge as a function of the plasma parameters. As an example, **Figure 12** shows the absorbed electron power density as a function of position and time during a single LF cycle in the α-γ regime (V_{RF} = 300 V, V_{LF} = 700 V and γ = 0.1). To simplify the analysis, the total electron power density is averaged over the RF cycle (**Figure 12b**) and compared to the LF power density (**Figure 12c**). These figures clearly point out the RF power absorption density in the plasma bulk and the LF power absorption density related to electron avalanche in the cathode sheath during the γ phase of the discharge.

The total time-averaged power density absorbed by the electrons is

$$P_{TOTAL} = -e\langle \Gamma_e E \rangle_t \quad \textbf{(7)}$$

where E is the electric field, Γ_e is the electron flux, and $-e$ is the electron charge. The LF contribution to this power density, shown in **Figure 12c,** is calculated from the RF-averaged electric field and electron flux according to:

$$P_{LF} = -e\langle \langle \Gamma_e \rangle_{RF} \langle E \rangle_{RF} \rangle_t \quad \textbf{(8)}$$

It turns out that the LF power density can be negative in some part of the discharge near the anode (because the electrons diffuse against the electric force) but is always strongly positive in the cathode sheath due to the electron avalanche induced by secondary emission. Therefore, we assume that the power density absorbed by the secondary electron avalanches can be estimated from:

$$P_{LF}^{+} = \langle \max(-e\langle \Gamma_e \rangle_{RF} \langle E \rangle_{RF}, 0) \rangle_t \quad \textbf{(9)}$$

Similar expressions hold for the power absorbed by ions, and the LF power density turns out to be always positive in this case.

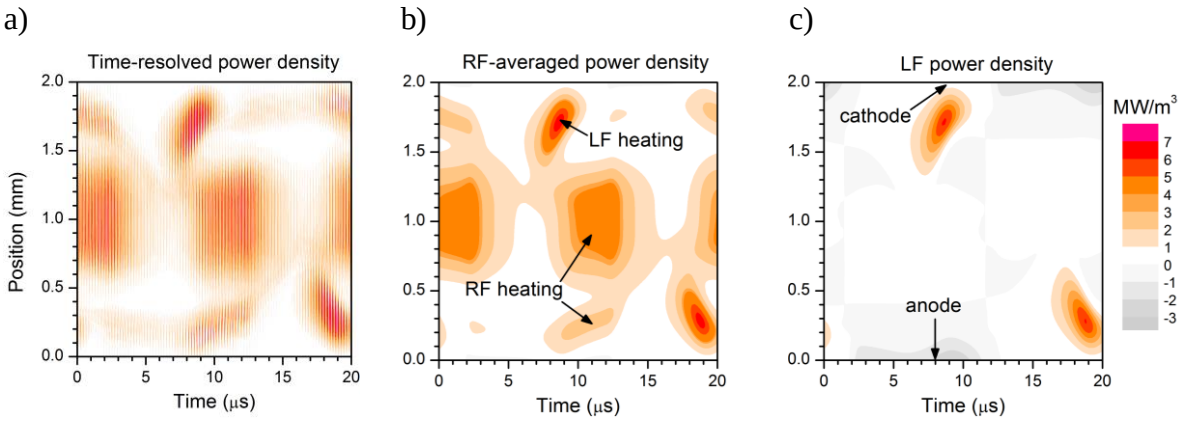

Figure 12. Simulated space and time variation of the power density absorbed by electrons during one LF cycle with V_{RF} = 300 V, V_{LF} = 700 V and γ = 0.1: a) RF-resolved power density $-e\Gamma_e E$, b) RF-averaged power density $-e\langle\Gamma_e E\rangle_{RF}$, c) LF component of power density $-e\langle\Gamma_e\rangle_{RF}\langle E\rangle_{RF}$, obtained from the RF-averaged electric field and RF-averaged electron flux.

The variation of the total absorbed power and its positive LF part, per electron and per ion, are presented in **Figure 13** for V_{RF} = 250, 300 and 350 V and for γ = 0.10 as a function of the LF voltage amplitude. These powers per electron/ion are defined as the ratio of the spatially-averaged power densities given above, to the spatially-averaged electron/ion density.

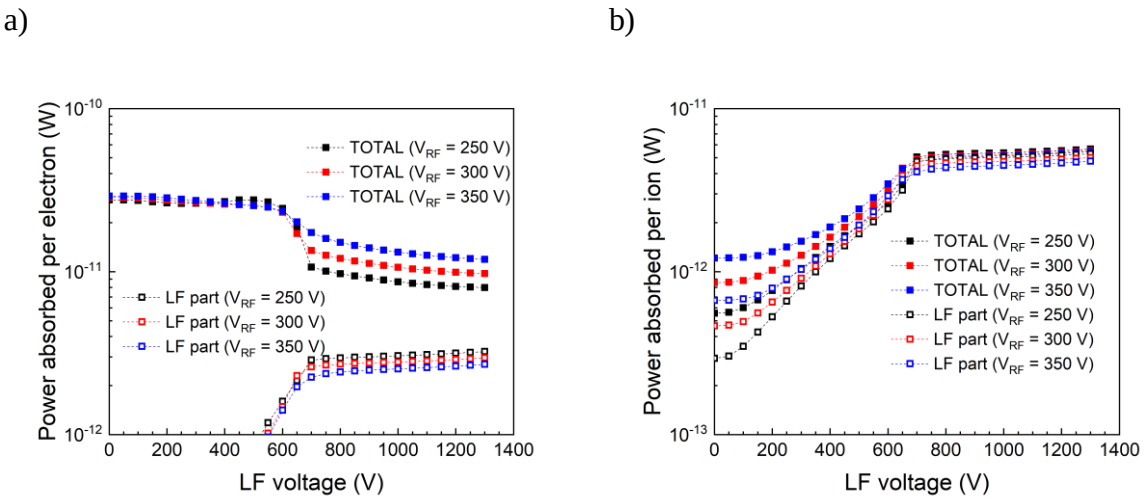

Figure 13. Absorbed power for V_{RF} = 250, 300 and 350 V and for γ = 0.10 as a function of the LF voltage amplitude per a) electron and b) ion

The total power absorbed per electron remains independent of the RF voltage amplitude until the V_{LF} transition threshold. The LF contribution to the power absorbed per electron increases

with V_{LF} but remains low. Clearly, the total power per electron is completely dominated by the RF heating (Total – LF part) even at high LF voltage. Three zones are observed as a function of the LF voltage amplitude. First of all, the total power absorbed per electron is constant and independent of the RF voltage amplitude, then it drastically decreases over 100 V at the transition, to finally decrease linearly once the α-γ-mode is reached. From the transition, the LF voltage amplitude makes electron heating less efficient likely because of the sheath thickness decrease. The power absorbed per ion is controlled by the LF voltage and increases with the LF voltage amplitude. It remains constant once the α-γ-mode is reached and the RF voltage dependence is less significant.

Conclusion

On the basis of experiments and modelling, a better understanding of the transition of the DF DBD from α to α-γ-mode [20] is achieved in an Ar-NH_3 Penning mixture. The parameters investigated in this study are the RF and LF voltage amplitude as well as the NH_3 concentration in the experiments and the γ coefficient in the modelling. All these parameters determine the ionization rate.

Emission spectroscopy measurements shown that the transition results in a drastic increase of the argon and NH emissions. For 133 ppm of NH_3, it is observed for V_{LF} higher than 400 V independently of the RF voltage amplitude. The increase of the NH_3 concentration leads to a decrease of the LF voltage amplitude required to reach the α-γ-mode. This last observation is explained by an increase of the ionization rate through the Penning reaction which enhance the ionization in the sheath.

The numerical model shows that the transition from α to α-γ-mode occurs when the sheath becomes self-sustained (ionization into the sheath > 1/ γ). Once the α-γ-mode is reached, the maximum of the gas voltage remains quasi-constant. It is independent of both LF and RF voltage amplitudes.

The secondary electron emission coefficient (γ) does not influence the α-mode but allows the transition to occur at lower LF voltage amplitude and lower gas voltage maximum. Without secondary electron emission, $\gamma = 0$, no transition from α to α-γ-mode takes place. For $\gamma > 0$, increasing the secondary electron emission coefficient yields a decrease of the LF voltage amplitude required to switch from α to α-γ-mode: 700 V for $\gamma = 0.05$, 600 V for $\gamma = 0.10$ and 550 V for $\gamma = 0.15$. The mean densities of particles are almost independent of the γ value except during the transition.

In the α-γ-mode, the power absorbed by electrons is mostly due to RF while the power absorbed per ion is due to LF. In the α-mode, the power absorbed per electron is independent of the RF and LF voltage amplitude while the power absorbed per ion drastically increases with the LF voltage amplitude. In the α-γ-mode, the LF voltage amplitude makes electron heating less efficient and the power absorbed per ion remains constant.

References

[1] U. Kogelschatz, “Dielectric Barrier Discharge : Their History, Discharge Physic, and Industrial Applications,” *Plasma Chem. Plasma Process.*, vol. 23, no. 1, pp. 1–46, 2003.

[2] F. Massines and G. Gouda, “A comparison of polypropylene-surface treatment by filamentary, homogeneous and glow discharges in helium at atmospheric pressure,” *J. Phys. D. Appl. Phys.*, vol. 31, no. 24, pp. 3411–3420, 1998.

[3] M. Gelker, C. C. Müller-Goymann, and W. Viöl, “Permeabilization of human stratum corneum and full-thickness skin samples by a direct dielectric barrier discharge,” *Clin. Plasma Med.*, vol. 9, pp. 34–40, 2018.

[4] B. Dong, J. Bauchire, J. Pouvesle, P. Magnier, and D. Hong, “Experimental study of a DBD surface discharge for the active control of subsonic airflow,” *J. Phys. D. Appl. Phys.*, vol. 41, 2008.

[5] P. Brunet, R. Rincón, Z. Matouk, M. Chaker, and F. Massines, “Tailored Waveform of Dielectric Barrier Discharge to Control Composite Thin Film Morphology,” *Langmuir*, vol. 34, no. 5, pp. 1865–1872, 2018.

[6] Q. H. Trinh, M. M. Hossain, S. H. Kim, and Y. S. Mok, “Tailoring the wettability of glass using a double-dielectric barrier discharge reactor,” *Heliyon*, vol. 4, no. 1, p. e00522, 2018.

[7] B. Ghimire, D. P. Subedi, and R. Khanal, “Improvement of wettability and absorbancy of textile using atmospheric pressure dielectric barrier discharge,” *Cit. AIP Adv.*, vol. 7, no. 085213, 2017.

[8] O. Levasseur, M. Vlad, J. Profili, N. Gherardi, A. Sarkissian, and L. Stafford, “Deposition of fluorocarbon groups on wood surfaces using the jet of an atmospheric-pressure dielectric barrier discharge,” *Wood Sci. Technol.*, vol. 51, no. 6, pp. 1339–1352, 2017.

[9] J. Profili, O. Levasseur, J. B. Blaisot, A. Koronai, L. Stafford, and N. Gherardi, “Nebulization of Nanocolloidal Suspensions for the Growth of Nanocomposite Coatings in Dielectric Barrier Discharges,” *Plasma Process. Polym.*, vol. 13, no. 10, pp. 981–989, 2016.

[10] R. Bazinette, J. F. Lelièvre, L. Gaudy, and F. Massines, “Influence of the Discharge Mode on the Optical and Passivation Properties of SiNx:H Deposited by PECVD at Atmospheric Pressure,” *Energy Procedia*, vol. 92, pp. 309–316, 2016.

[11] J. Vallade *et al.*, “A-SiNx:H antireflective and passivation layer deposited by atmospheric pressure plasma,” *Energy Procedia*, vol. 27, pp. 365–371, 2012.

[12] R. Bazinette, J. Paillol, J. F. Lelièvre, and F. Massines, “Atmospheric Pressure Radio-Frequency DBD Deposition of Dense Silicon Dioxide Thin Film,” *Plasma Process. Polym.*, vol. 13, no. 10, pp. 1015–1024, 2016.

[13] F. Massines *et al.*, “Hydrogenated Silicon Nitride SiNx:H Deposited by Dielectric Barrier Discharge for Photovoltaics,” *Plasma Process. Polym.*, vol. 13, no. 1, pp. 170–183, 2016.

[14] R. Bazinette, J. Paillol, and F. Massines, “Optical emission spectroscopy of glow, Townsend-like and radiofrequency DBDs in an Ar/NH3mixture,” *Plasma Sources Sci. Technol.*, vol. 24, no. 5, 2015.

[15] J. J. Shi, D. W. Liu, and M. G. Kong, “Plasma stability control using dielectric barriers in radio-frequency atmospheric pressure glow discharges,” *Appl. Phys. Lett.*, vol. 89, no. 8, pp. 8–10, 2006.

[16] J. J. Shi and M. G. Kong, “Mode transition in radio-frequency atmospheric argon discharges with and without dielectric barriers,” *Appl. Phys. Lett.*, vol. 90, no. 10, 2007.

[17] F. R. Kong, Z. L. Zhang, and B. H. Jiang, “Numerical study of the discharge properties of atmospheric dielectric barrier discharge by using 200 kHz/13.56 MHz excitations,” *AIP Adv.*, vol. 8, no. 7, 2018.
[18] L. Bischoff *et al.*, “Experimental and computational investigations of electron dynamics in micro atmospheric pressure radio-frequency plasma jets operated in He / N 2 mixtures,” 2018.
[19] Z. L. Zhang, J. W. M. Lim, Q. Y. Nie, X. N. Zhang, and B. H. Jiang, “Electron heating and mode transition in dual frequency atmospheric pressure argon dielectric barrier discharge,” *AIP Adv.*, vol. 7, no. 10, p. 105313, 2017.
[20] R. Magnan, G. Hagelaar, M. Chaker, and F. Massines, “Atmospheric pressure dual RF-LF frequency discharge : in fl uence of LF voltage amplitude on the RF discharge behavior,” *Plasma Sources Sci. Technol.*, vol. 29, no. 3, p. 35009, 2020.
[21] J. E. Chilton, J. B. Boffard, R. S. Schappe, and C. C. Lin, “Measurement of electron-impact excitation into the 3 p 5 4 p levels of argon using Fourier-transform spectroscopy,” vol. 57, no. 1, pp. 267–277, 1998.
[22] J. B. Boffard, G. A. Piech, M. F. Gehrke, L. W. Anderson, and C. C. Lin, “Measurement of electron-impact excitation cross sections out of metastable levels of argon and comparison with ground-state excitation,” vol. 59, no. 4, 1999.
[23] Y. P. Raizer, *Gas discharge Physics*. 1991.